

# Thermodynamics and Kinetics of CO<sub>2</sub> Adsorption on Dehydrated Palladium/Cobalt-Based Cyanogels: A Highly Selective, Fully Reversible System for CO<sub>2</sub> Storage

Rahul S. Deshpande, Stefanie L. Sharp-Goldman, and Andrew B. Bocarsly\*

Department of Chemistry, Frick Laboratory, Princeton University,  
Princeton, New Jersey 08544

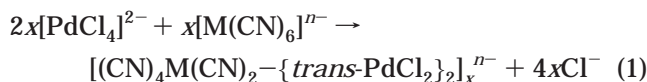
Received April 9, 2002. In Final Form: July 1, 2002

Carbon dioxide is selectively adsorbed on cyanide-bridged palladium/cobalt gels, synthesized from aqueous solutions of Na<sub>2</sub>PdCl<sub>4</sub> and K<sub>3</sub>[Co(CN)<sub>6</sub>]. The cyanide bridges, connecting the palladium and cobalt metal centers, are characteristic of these gels; hence, these gels are termed *cyanogels*. The thermodynamics and kinetics of the CO<sub>2</sub> adsorption and desorption processes on aerogels and xerogels formed from Pd/Co cyanogels are analyzed here. Aerogel versus xerogel structures have a profound effect on the thermodynamics and kinetics of CO<sub>2</sub> adsorption. The CO<sub>2</sub> adsorption process is fully reversible on both types of gels discussed. The gas adsorption capacity of the aerogel exceeds that of the xerogel by a factor of slightly over two. From the ease and reproducibility of the CO<sub>2</sub> desorption and the associated enthalpy values, it is concluded that CO<sub>2</sub> is physisorbed on these gels. The kinetics of adsorption and desorption are analyzed: both processes are first-order in the gels.

## Introduction

One of the ways of synthesizing porous materials is by solution sol–gel processing,<sup>1–4</sup> the formation of a gel from a reaction between molecular precursors in solution, followed by the removal of the solvent. Via sol–gel processing, one has the ability to control the properties of the bulk product by manipulating those of the molecular precursors. Among its significant advantages over the conventional “powder” route to porous materials are lower material processing temperatures and the ability to form ultrahomogeneous and multicomponent systems. In addition, the porous materials need not be monolithic: rheological properties of the sols and gels allow the formation of films, fibers, and composites by techniques such as spinning, dip coating, or impregnation.<sup>1,2</sup>

We have reported<sup>5</sup> that aqueous solutions of the square planar complexes Na<sub>2</sub>PdCl<sub>4</sub> and K<sub>x</sub>[M(CN)<sub>n</sub>], with  $n = 4–8$  and M as a transition metal, react to form gelled polymeric systems as shown by the equation



The product polymer is characterized by the presence of bridging cyanide ligands between the Pd(II) and M metal centers, forming a star-polymer system.<sup>6</sup> Polymerization occurs via the substitution of two chloride ligands, *trans* to each other, on the Pd(II) centers, by the nitrogen end of the cyanide ligands on the M metal center, to generate

an extended cyanide-bridged structure. Since the cyanide bridges are central to these gels and distinguish them from classic metal–oxo gels, we refer to these gels, generically, as *cyanogels*.

The hydrogels obtained on mixing the aqueous transition metal reagent solutions are typically ~95% water by mass. From these, aero- or xerogels are obtained depending on the solvent removal process employed. A supercritical CO<sub>2</sub> extraction of the solvent yields the aerogel,<sup>7</sup> while the xerogel is obtained by direct evaporation of the aqueous phase at 95 °C and ambient pressure.<sup>7</sup> These two forms of cyanogels, of the same composition, vary in density and bulk morphology, which suggests a structural difference arising largely from the dissimilar drying processes.

In this paper, we discuss and analyze the thermodynamics and kinetics of selective and reversible CO<sub>2</sub> adsorption and desorption processes on palladium/cobalt (Pd/Co)-based cyanogels. Thermodynamic parameters such as the isosteric enthalpy and entropy, the equilibrium constant, and the standard free energy for the CO<sub>2</sub> adsorption on these Pd/Co cyanogels are calculated. The rate constants for both CO<sub>2</sub> adsorption and desorption are obtained.

The selective adsorption of CO<sub>2</sub> by the cyanogels can be harnessed practically in at least two principal ways: by using the cyanogels as reservoirs for trapping CO<sub>2</sub> reversibly and by constructing filters having an embedded layer of the gels. The former may be utilized in enclosed areas where a high CO<sub>2</sub> concentration would be detrimental to health. The reversibility of the adsorption also promotes the reuse of these reservoirs, circumventing the severe limitation of present CO<sub>2</sub> adsorbents that irreversibly form carbonates. Gel-embedded filters can be used to separate mixtures of gases on the basis of the differential adsorption propensities of the gases. This suggests an interesting application in the trapping and removal of greenhouse emissions from industrial sources.

(7) Sharp, S. L. Ph.D. Thesis, Princeton University, Princeton, NJ, 2000.

\* Corresponding author. (609)-258-3888; bocarsly@princeton.edu.

(1) Livage, J.; Henry M.; Sanchez, C. *Prog. Solid State Chem.* **1988**, *18*, 259–341.

(2) Brinker, C. J.; Scherer, G. W. *Sol–Gel Science: The Physics and Chemistry of Sol–Gel Processing*; Academic Press: Boston, MA, 1990.

(3) Cheetham, A. K.; Brinker, C. J. *Materials Society Symposium Proceedings*; San Francisco, CA, 1994.

(4) Jones, R. W. *Fundamental Principles of Sol–Gel Technology*; The Institute of Metals: London, 1989.

(5) Pfennig, B. W.; Bocarsly, A. B.; Prud'homme, R. K. *J. Am. Chem. Soc.* **1993**, *115*, 2661–2665.

(6) Heibel, M. Ph.D. Thesis, University of Ljubljana, Ljubljana, Slovenia, 1996.

## Experimental Section

The gels studied in this paper were synthesized from aqueous solutions of sodium tetrachloropalladate(II), Na<sub>2</sub>PdCl<sub>4</sub>, and potassium hexacyanocobaltate(III), K<sub>3</sub>[Co(CN)<sub>6</sub>], in a 2:1 volume ratio, respectively, at room temperature. The starting chemicals were reagent grade: the former was obtained from Pressure Chemicals Inc., and the latter, from Aldrich Inc. Both were used as received. In-house deionized, osmotically purified water was used for all the solutions.

A typical hydrogel was synthesized by a 2:1 volumetric reaction between 60 mM solutions of Na<sub>2</sub>PdCl<sub>4</sub> and K<sub>3</sub>[Co(CN)<sub>6</sub>], which provides a stoichiometric ratio.<sup>5</sup> Such a gel is referred to as a 60 mM Pd/Co cyanogel.

Mixing the reactants together resulted in a dark orange solution that, over time, increased in viscosity. This solution underwent a well-defined sol-gel transition, and a polymeric gel, consisting of cyanide-bridged palladium/cobalt centers, formed between the walls of the container. Aging of the gels, which normally takes one week, was carried out at room temperature. Thermogravimetric analysis of the hydrogel revealed that it was composed of 99% water immediately on formation and eventually stabilized at ~95% water. The water of gelation was eliminated by smearing out the gel on filter paper and drying it overnight in an oven at 95 °C. The resulting xerogel was rinsed with distilled water to remove the salts produced during the reaction, dried again in the oven, and then mechanically powdered.

Aerogels were made by, first, exchanging the water of the hydrogel with acetone by placing the gel in an acetone bath. The bath was changed twice daily for 3 days to ensure that all the water in the gel was replaced by acetone. The acetone-impregnated gel was then placed in a computer-controlled autoclave (CF Technologies, CFT-AD-50, 600 mL volume), and the acetone was exchanged with CO<sub>2</sub> (BOC gases, 99.99% purity). The autoclave was flushed five times with CO<sub>2</sub> to ensure a complete exchange of acetone with CO<sub>2</sub>. It was then brought up to 9 MPa and 45 °C to render the CO<sub>2</sub> supercritical. The supercritical CO<sub>2</sub> was then extracted from the aerogel by bringing the autoclave to ambient pressure conditions.

Carbon dioxide (99.99%), nitrogen (99.99%), and argon (99.99%), obtained from BOC gases, were used as received. Thermogravimetric analyses were performed with a Perkin-Elmer thermogravimetric analyzer TGA 7 with pressures ranging from 8 to 65 psi under an N<sub>2</sub> or Ar atmosphere. At room temperature, in this pressure range, the gels adsorb only CO<sub>2</sub>; pure N<sub>2</sub> and Ar were used to desorb the adsorbed CO<sub>2</sub>. The temperature program used for a gravimetric analysis consisted of three distinct steps: heating the sample from 35 to 120 °C at the rate 6 °C/min, holding the temperature constant at 120 °C for 15 min, and cooling to 35 °C at the rate 10 °C/min. All the steps were carried out under a pure Ar or N<sub>2</sub> atmosphere. All subsequent adsorption analyses in the TGA were performed at 35 °C. Calorimetric analyses were recorded using a Perkin-Elmer differential scanning calorimeter, DSC 7. The flows of gases into the TGA 7 or the DSC 7 were monitored by a flow meter (Aalborg, model 042-15). Nitrogen and carbon dioxide sorption data were collected on a Micrometrics ASAP 2010. The N<sub>2</sub> adsorption isotherms were measured at 77 K, while the ones with CO<sub>2</sub> were recorded at 0 °C in the pressure range 10<sup>-6</sup> to 1.1 atm.

**Warning:** Hazardous gases, HCN and (CN)<sub>2</sub>, can be evolved during heating of the gels above ~200 °C. Therefore, while doing the thermogravimetric and calorimetric analyses, it is important to trap these product gases using a series of aqueous bubblers: the first one should contain bleach while the terminal one contains sodium hydroxide.

## Results and Discussion

For the cyanogels discussed in this paper, the densities of the aero- and xerogels, respectively, are 0.28 and 2.25 g/cm<sup>3</sup> as measured by helium pycnometry. Application of the BET isotherm to the nitrogen adsorption data yields surface areas of 800 m<sup>2</sup>/g for the aerogel and 450 m<sup>2</sup>/g for the xerogel.

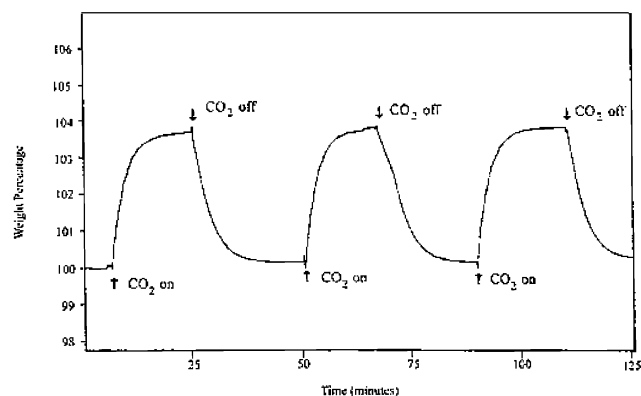


**Figure 1.** CO<sub>2</sub>/Ar recycling for the 60 mM Pd/Co xerogel illustrating the complete reversibility of CO<sub>2</sub> adsorption and its reproducibility.

**Table 1.** Adsorption of Different Gases by the Cyanogels

gas	aerogel	xerogel
CO <sub>2</sub> , N <sub>2</sub> O	9%	4%
SF <sub>6</sub>	11%	a
N <sub>2</sub> , Ar, O <sub>2</sub> , CH <sub>4</sub>	a	a

<sup>a</sup> Not adsorbed.

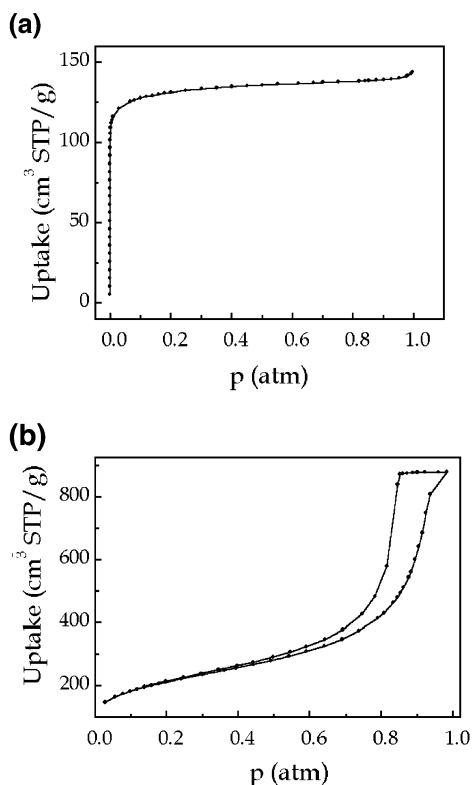
Figure 1 shows the gravimetric profile of the adsorption of pure CO<sub>2</sub> on a powdered sample of 60 mM Pd/Co xerogel. Ar was used to desorb the adsorbed CO<sub>2</sub>. The pressures of both the gases were kept constant at 20 psi. As this figure illustrates, the xerogel adsorbs about 4% CO<sub>2</sub> by mass and the adsorption is completely reversible at 35 °C. While Figure 1 shows three CO<sub>2</sub>/Ar cycles, this cycling was carried out 10 times with almost no change, indicating that the adsorption process is reversible and reproducible. Pd/Co aerogels show a similar adsorption profile; however, they take up about 9% CO<sub>2</sub> by mass.

Table 1 lists the amounts of different gases adsorbed by the cyanogels. As it indicates, aerogels adsorb more than the xerogels. The increased gas uptake by the aerogel is in line with its more expanded structure vis-à-vis the xerogel and its larger average pore size. Another indication of the smaller pore dimensions of the xerogel is provided by the fact that only the aerogel adsorbs SF<sub>6</sub>. This being a bigger molecule than CO<sub>2</sub>, for instance, it cannot penetrate the micropores of the xerogel and, hence, there is no SF<sub>6</sub> adsorption on the xerogel; the aerogel, in contrast, adsorbs 11% by weight. Neither of the gels adsorb Ar, N<sub>2</sub>, O<sub>2</sub>, or CH<sub>4</sub>; these gases, therefore, are suitable candidates for desorbing the adsorbed gases off the gels.

**Thermodynamics of CO<sub>2</sub> Adsorption.** The adsorption isotherms for representative aero- and xerogels are shown in Figure 2. The xerogel, Figure 2a, shows a distinct type I isotherm,<sup>8</sup> indicating that it is almost purely microporous. The aerogel, Figure 2b, on the other hand, yields a type IV isotherm,<sup>8</sup> characteristic of a mesoporous solid.

The enthalpies of CO<sub>2</sub> adsorption on the 60 mM Pd/Co aero- and xerogel were measured experimentally by differential scanning calorimetry under CO<sub>2</sub>. The values are  $-23 \pm 2$  and  $-37 \pm 3$  kJ/mol of CO<sub>2</sub> adsorbed for the aero- and xerogel, respectively. From the reversibility of the adsorption as well as the value of the enthalpy, it can be concluded that CO<sub>2</sub> is physisorbed onto the aerogel; the adsorption isotherm indicates capillary condensation in the aerogel. The low-pressure saturation and repro-

(8) Sing, K. S. W.; Everett, D. H.; Haul, R. A. W.; Moscou, L.; Pierotti, R. A.; Rocquero, J.; Siemieniowska T. *Pure Appl. Chem.* **1985**, 603.



**Figure 2.** (a) CO<sub>2</sub> adsorption isotherm for the 60 mM Pd/Co xerogel. Note the distinct type I behavior indicative of the predominant microporosity of the gel. (b) CO<sub>2</sub> adsorption isotherm for the Pd/Co aerogel displaying the type IV behavior characteristic of mesoporous solids.

ducible reversibility of CO<sub>2</sub> adsorption on the xerogel, as depicted in Figure 1, also point to a physisorption process. The enthalpy of CO<sub>2</sub> adsorption is higher for the xerogel than that for the aerogel despite the fact that the latter adsorbs over twice as much CO<sub>2</sub> than the former. The reason for this apparent discrepancy is intimately linked to the structure of these gels, specifically to the micropore versus mesopore nature of the xero- and aerogel, respectively.

The CO<sub>2</sub> adsorption in the xerogel takes place in micropores that, on average, have a radius of ~1 nm.<sup>9</sup> In such narrow pores, the potential fields from the neighboring walls overlap significantly, thereby enhancing the interaction potential between the pore walls and the adsorbate molecules.<sup>10–12</sup> The steep initial part of the isotherm, indicating that >75% of the pore volume is filled at  $p < 0.1$  atm, is a manifestation of the high fields present within these micropores. This enhancement of the interaction potential leads to an increased enthalpy of CO<sub>2</sub> adsorption for the xerogel when compared to that of the aerogel. Additional evidence of the enhancement of the interaction potential within the micropores of the xerogel comes from the relative values of the rate constants for the desorption processes on these gels, as discussed in the section on kinetics that follows.

(9) Gregg, S. J.; Sing, K. S. W. *Adsorption, Surface Area and Porosity*, 2nd ed.; Academic Press: London, 1982.

(10) Everett, D. H.; Powl, J. C. *J. Chem. Soc., Faraday Trans. 1* **1976**, 72, 619.

(11) Maitland, G. C.; Rigby, M.; Smith, E. B.; Wakeham, W. A. *Intermolecular Forces: Their Origin and Determination*, Clarendon: Oxford, 1981.

(12) Steele, W. A. *The Interactions of Gases with Solid Surfaces*; Pergamon: Oxford, U.K., 1973.

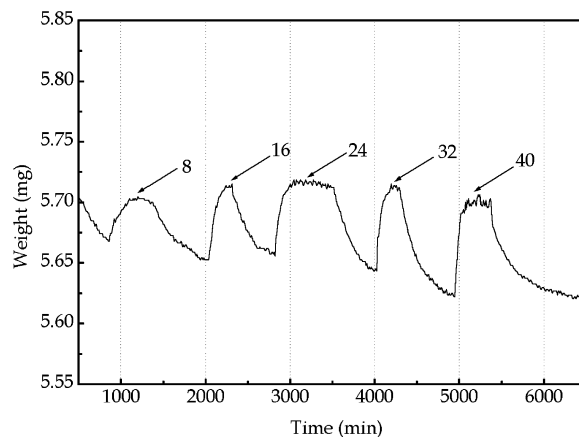


**Figure 3.** Thermogravimetric profile of CO<sub>2</sub> adsorption on the 60 mM Pd/Co xerogel. Numbers show the CO<sub>2</sub> pressures in psi.

In the case of the aerogel, on the other hand, the average pore diameter is  $9 \pm 1$  nm, as computed from the desorption branch of the N<sub>2</sub> isotherm using the BJH method.<sup>13</sup> Once the monolayer is formed on the pore walls, the adsorption takes place primarily by a cooperative condensation process between molecules,<sup>9</sup> as in a typical physisorption, rather than by an enhancement of the interaction potential. The enthalpy of adsorption, therefore, is of the order of 20 kJ/mol.

**Adsorption and Desorption Kinetics.** Figure 3 shows the gravimetric profile for the CO<sub>2</sub> adsorption and desorption from a 60 mM Pd/Co xerogel as a function of CO<sub>2</sub> partial pressure. As the xerogel does not adsorb N<sub>2</sub> at this temperature, dry N<sub>2</sub> was used for the CO<sub>2</sub> desorption. While the figure shows CO<sub>2</sub> partial pressure changes from 8 to 40 psi, the pressures were varied from 8 to 65 psi. As the figure illustrates, the slope of the leading edge of the adsorption curve increases monotonically with CO<sub>2</sub> partial pressure. The kinetics of adsorption would be expected to depend on the partial pressure of the gas. The monotonic increase in the slopes of the leading edges of the adsorption curves with CO<sub>2</sub> partial pressure confirms this expectation.

The detailed kinetics of the CO<sub>2</sub> adsorption and desorption processes for a 60 mM Pd/Co xerogel are illustrated in Figure 4. The evolution of the fraction of vacant adsorption sites in the gel, at different CO<sub>2</sub> partial pressures, as the adsorption proceeds, is shown in part a, while part b shows the time dependence of the fraction of occupied sites as the desorption progresses.

In terms of the Langmuir adsorption model,<sup>14</sup>

$$\theta = \frac{Kp}{1 + Kp} \quad (2)$$

(where  $\theta$  is the fraction of occupied adsorption sites,  $K$  is the equilibrium constant for the adsorption process, and  $p$  is the gas pressure), the fraction of vacant adsorption sites in part a corresponds to  $1 - \theta$ .

Assuming the xerogel to be an ensemble of adsorption sites, let  $n_a$  be the *actual* number of adsorption sites occupied by the adsorbate molecules on the xerogel at a given time,  $n_t$  be the *total* number of adsorption sites,  $n_g$  be the number of adsorbate molecules adsorbed at a given time,  $n_s$  be the number adsorbed at saturation, and  $n$  be the number of adsorption sites required by each molecule of the adsorbate on the xerogel.

(13) Barrett, E. P.; Joyner, L. G.; Halenda, P. H. *J. Am. Chem. Soc.* **1951**, 73, 373.

(14) Langmuir, I. *J. Am. Chem. Soc.* **1915**, 37, 1139.

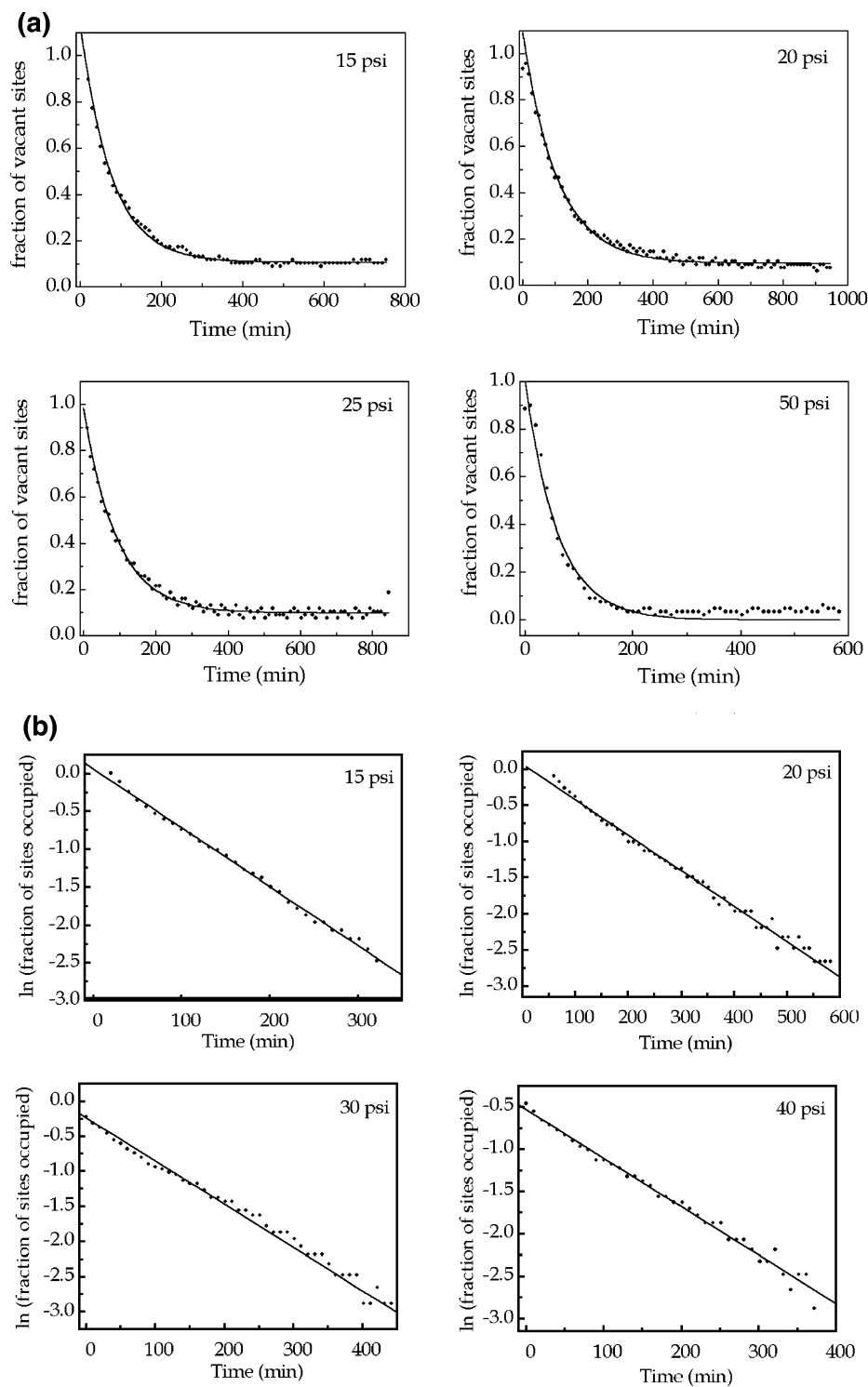


**Figure 4.** (a) Time profile of the decay of the fraction of vacant adsorption sites in the xerogel as the adsorption proceeds for four representative CO<sub>2</sub> pressures. All the plots fit a first-order exponential decay. CO<sub>2</sub> pressures are indicated in the top right-hand corner in all the plots. (b) Log plot of the decay of the fraction of filled adsorption sites in the xerogel as the desorption progresses for four representative CO<sub>2</sub> pressures.

Then, assuming that  $n$  does not change, as the adsorption progresses

$$n_a = n_g n \quad \text{and} \quad n_t = n_s n \quad (3)$$

Both  $n_a$  and  $n_t$  are dependent on  $n$ , but their ratio, which can be interpreted as the fraction of sites occupied, is independent of  $n$ . The difference of this ratio from unity is the fraction of vacant sites. The numbers  $n_g$  and  $n_s$  can both be obtained from the gravimetric profile of the adsorption.

As the adsorption proceeds, the fraction of vacant sites decreases. The time dependence, observed in Figure 4a, is well described by a process that is solely first-order in  $1 - \theta$ , the fraction of vacant sites, as demonstrated by the solid line fits to the data. Averaged over all pressures studied, the mean "goodness of fit" parameter,  $R^2$ , is 0.98; the mean rate constant for adsorption is  $(2.1 \pm 0.2) \times 10^{-1} \text{ s}^{-1} \text{ atm}^{-1}$ . Within experimental error, the observed rate constant is unchanged with pressure over the entire range studied (0.54–4.4 atm), suggesting that the adsorption

**Table 2. Thermodynamic and Kinetic Data for the Cyanogels**

type of gel	$k_{\text{adsorption}}$ ( $\text{s}^{-1} \text{atm}^{-1}$ )	$k_{\text{desorption}}$ ( $\text{s}^{-1}$ )	$K_{\text{eq}}^a$ ( $\text{atm}^{-1}$ )	$\Delta H^\circ$ (kJ/mol)	$\Delta G^\circ$ (kJ/mol)	$\Delta S^\circ$ (J/mol K)
aerogel	$(2.9 \pm 0.3) \times 10^{-1}$	$(1.8 \pm 0.2) \times 10^{-2}$	$16 \pm 3$	$-23 \pm 2$	$-6.9 \pm 0.8$	$-54 \pm 3$
xerogel	$(2.1 \pm 0.2) \times 10^{-1}$	$(6.6 \pm 0.9) \times 10^{-3}$	$30 \pm 7$	$-37 \pm 3$	$-8.4 \pm 0.9$	$-96 \pm 4$

$$^a K_{\text{eq}} = k_{\text{adsorption}}/k_{\text{desorption}} = \theta/[(1 - \theta)p].$$

mechanism is invariant under these conditions. Since only one kinetic process is observed over the whole pressure range, and the isotherm for this material shows monolayer adsorption up to 1 atm, it appears that the xerogel only exhibits monolayer adsorption over the whole pressure range investigated.

Similarly, the desorption is well described as a process that is solely first-order in the fraction of occupied sites,  $\theta$  (see Figure 4b). The fits to these data (solid lines in Figure 4b) yield  $R^2$  values of 0.97. The mean rate constant for desorption is  $(6.6 \pm 0.9) \times 10^{-3} \text{ s}^{-1}$ , indicating that the desorption process is first-order in the fraction of filled sites in the xerogel as well.

For the aerogels, a reasoning similar to the one above applies. The only difference between the adsorption on the xerogel and that on the aerogel is that, in the case of the former, the adsorption is largely limited to a monolayer, while, in the case of the latter, the adsorption is multilayer. The total and the actual numbers of gas molecules adsorbed,  $N_T$  and  $N_A$ , respectively, can be calculated from the gravimetric data. As adsorption proceeds, the difference  $N_T - N_A$  decreases, and hence, so does the ratio  $(N_T - N_A)/N_T$ . As desorption progresses,  $N_A$  decreases, and so does  $N_A/N_T$ . The ratio  $(N_T - N_A)/N_T$ , similar to  $1 - \theta$  for the xerogels, can be interpreted as the fraction of vacant adsorption sites on the aerogels, while  $N_A/N_T$  relates to the fraction of occupied adsorption sites. The time dependence of both of these ratios for Pd/Co aerogels displays characteristics similar to those of the fractions of vacant and filled adsorption sites for the xerogels, respectively. Both fit well to a first-order exponential decay with a mean "goodness of fit" parameter of 0.96.

Table 2 lists the rate constants for the adsorption and desorption processes for the aero- and xerogels. While the  $\text{CO}_2$  adsorption rate constants for both types of gels are comparable, the desorption rate constant for the xerogel is almost 3 times lower than that for the aerogel (cf. Table 2). This implies that the adsorbate molecules are more tightly bound to the adsorbent, consistent with the increased interaction potential within the micropores.

From a knowledge of the adsorption and desorption rate constants, the equilibrium constant for the adsorption process can be arrived at. There are, in fact, two independent ways of estimating the equilibrium constant for the  $\text{CO}_2$  adsorption on the cyanogels. One is by taking the ratios of the adsorption and desorption rate constants, while the other is from the slope and intercept of the linear fit based on the Langmuir model to the adsorption data. According to the Langmuir model, the ratio of the slope to the intercept of the linear fit to the adsorption data yields the equilibrium constant. Using the former approach, for the aerogel, the value of the equilibrium constant at room temperature is  $16 \pm 3 \text{ atm}^{-1}$ , while, from the latter, it is  $19 \pm 4 \text{ atm}^{-1}$ . For the xerogel, the equilibrium constant values are  $30 \pm 7 \text{ atm}^{-1}$  by the first

method and  $25 \pm 5 \text{ atm}^{-1}$  by the second. The agreement of the values of the equilibrium constant obtained by these two independent methods for both the aero- and xerogels is gratifying and provides a corroboration of the values of the equilibrium constant. The equilibrium constant, in turn, enables a calculation of the free energy change for adsorption. The free energy and the enthalpy changes during the adsorption process lead to an estimation of the entropy of adsorption.<sup>15</sup> Table 2 lists all these thermodynamic parameters.

The entropy change of  $\text{CO}_2$  adsorption on the xerogel is significant; it is of the order of the molar entropy change associated with the condensation of water. The standard free energy change for the adsorption of  $\text{CO}_2$  on the aerogel is small. This indicates that the adsorption process is almost at equilibrium. The reproducible and complete reversibility of the  $\text{CO}_2$  adsorption is a manifestation of this small standard free energy change. The corresponding value for the xerogel is higher than that for the aerogel; this is consistent with a higher interaction potential between the adsorbate and adsorbent molecules in the micropores of the xerogel.

## Conclusions

We have analyzed the thermodynamics and kinetics of  $\text{CO}_2$  adsorption on the Pd/Co aero- and xerogels. The method of solvent removal plays a critical role in defining the structure and thereby the properties of these gels. This difference in structure manifests in three important properties of these cyanogels: gas-adsorption isotherms, isosteric heats of  $\text{CO}_2$  adsorption, and kinetics. The xerogel physisorbs 4%  $\text{CO}_2$  by mass, while the aerogel, because of its mesoporous structure, adsorbs 9% by the combined processes of physisorption and capillary condensation. The  $\text{CO}_2$  adsorption on both these types of gels is completely and reproducibly reversible. While the enthalpy of adsorption for the aerogel is typical of physisorption, it is distinctly higher for the xerogel because of an enhancement of the interaction potential within the micropores that leads to a stronger adsorbate-adsorbent association.

Both the adsorption and desorption processes are first-order with respect to the fractions of the vacant and occupied adsorption sites, respectively, on both these types of gels. The rate constant for  $\text{CO}_2$  desorption from the xerogel is almost 3 times smaller than the corresponding rate constant for the aerogel, indicative of the stronger interaction potential within the pores of the xerogel.

**Acknowledgment.** Financial support for this research from National Science Foundation Grant No. CHE-0079169 is gratefully acknowledged.

LA025821R